932 *Biochemistry* **2011,** *50,* 932–944
DOI: 10.1021/bi101583e

BIOCHEMISTRY
including biophysical chemistry & molecular biology
Article

Single-Stranded DNA Binding Proteins Unwind the Newly Synthesized Double-Stranded DNA of Model Miniforks[†]

Emmanuelle Delagoutte,*[,‡] Amélie Heneman-Masurel,[§] and Giuseppe Baldacci[‡]

[‡]*Institut Jacques Monod, UMR7592, "Pathologies de la réplication de l'ADN", CNRS and Université Paris-Diderot, Paris, France, and* [§]*Institut Curie, UMR 3348, "Stress génotoxiques et Cancer", CNRS and Université Paris-Sud 11, Paris, France*

Received September 30, 2010; Revised Manuscript Received December 8, 2010

ABSTRACT: Single-stranded DNA binding (SSB) proteins are essential proteins of DNA metabolism. We characterized the binding of the bacteriophage T4 SSB, *Escherichia coli* SSB, human replication protein A (hRPA), and human hSSB1 proteins onto model miniforks and double-stranded−single-stranded (ds−ss) junctions exposing 3′ or 5′ ssDNA overhangs. T4 SSB proteins, *E. coli* SSB proteins, and hRPA have a different binding preference for the ss tail exposed on model miniforks and ds−ss junctions. The T4 SSB protein preferentially binds substrates with 5′ ss tails, whereas the *E. coli* SSB protein and hRPA show a preference for substrates with 3′ ss overhangs. When interacting with ds−ss junctions or miniforks, the T4 SSB protein, *E. coli* SSB protein, and hRPA can destabilize not only the ds part of a ds−ss junction but also the daughter ds arm of a minifork. The T4 SSB protein displays these unwinding activities in a polar manner. Taken together, our results position the SSB protein as a potential key player in the reversal of a stalled replication fork and in gap repair-mediated repetitive sequence expansion.

Single-stranded DNA binding (SSB)[1] proteins are ubiquitous and essential proteins involved in multiple aspects of DNA metabolism (for reviews, see refs (*1*−*6*)). The primary function of SSB proteins is to cover naked single-stranded (ss) DNA exposed by helicases or nucleases to prevent secondary structure formation or nuclease digestion. During replication or nucleotide excision repair, the ss DNA covered by SSB proteins becomes the substrate for DNA polymerases. During homologous recombination-dependent DNA double-stranded (ds) break repair, SSB proteins bind first the 3′ ss overhang generated after ds break resection before being replaced by the recombinase RecA/Rad51. Recently, two new human SSB proteins, hSSB1 and hSSB2, with specific functions in DNA damage response were discovered (*7*, *8*). In addition to their protective role against nuclease attack and secondary structure formation, SSB proteins bind multiple protein partners and facilitate the assembly of genome maintenance complexes by coordinating their activities.

SSB proteins were initially called DNA "melting" or "helix destabilizing" proteins because they were able to perturb the melting transition of sequence specific polynucleotides, especially poly{d(A-T)}, but not a number of different natural DNAs (*9*). However, unwinding of random sequence duplexes of various lengths has been described for a number of SSB proteins, and this activity is ATP-independent, influenced by the monovalent and divalent salt concentrations, and requires a saturating amount of proteins (*10*−*15*). Local breathing of the ds DNA helix may create a nucleation site for the SSB proteins (*16*, *17*). As indicated by its acronym, the SSB protein binds ss DNA in a sequence-independent manner and covers ss DNA very efficiently. High affinity for ss DNA can be achieved in different ways. For example, the major human SSB protein, replication protein A or hRPA, binds ss DNA with an intrinsic binding constant of 0.01−1 nM and a cooperativity parameter ω of 10−20 (see ref *2* and references cited therein). On the other hand, a low intrinsic binding constant (in the micromolar range) combined with a high cooperativity (ω of 500−1000) allows bacteriophage T4 SSB protein to bind ss DNA very efficiently (ref *18* and references cited therein). In contrast, the bacteriophage T7 SSB protein binds ss DNA with an apparent binding constant in the micromolar range without any apparent cooperativity (*19*, *20*). Recent data suggest that T7 SSB protein efficiently finds its ss DNA target by prebinding and sliding along ds DNA (*21*). Sliding along ds DNA might also be a property of T4 SSB protein (*22*). Like T7 SSB protein, the recently discovered hSSB1 binds ss DNA with a low apparent binding constant (micromolar range) (*7*).

Structural studies suggest that the T4 SSB protein binds ss DNA as a monomeric protein of 33.5 kDa (*23*, *24*). The 18.8 kDa *Escherichia coli* SSB protein can assemble into a homotetramer or homo-octamer and wind the ss DNA around itself, organizing ss DNA in nucleosome-like units (*25*). The eukaryotic SSB protein, RPA, is a heterotrimeric protein that consists of three proteins of approximately 70, 32, and 14 kDa (p70, p32, and p14, respectively). Such a hetero-oligomeric structure can facilitate interactions with multiple binding partners, especially repair enzymes. Multi-RPA systems are universal in eukaryotes (*5*).

[†]This work was supported by the CNRS, Institut Curie, Institut Jacques Monod, and Université 7 Paris Diderot.

*To whom correspondence should be addressed: Institut Jacques Monod, UMR7592, "Pathologies de la réplication de l'ADN", CNRS and Université 7 Paris Diderot, Bâtiment Buffon, 15 Rue Hélène Brion, 75205 Paris cedex 13, France. Phone: 33 (0)1 57 27 80 73. Fax: 33 (0) 1 57 27 81 35. E-mail: delagoutte.emmanuelle@ijm.univ-paris-diderot.fr.

[1]Abbreviations: aRPA, alternative RPA; ds, double-stranded; DTT, dithiothreitol; EDTA, ethylenediaminetetraacetic acid; IPTG, isopropyl β-D-thiogalactoside; hRPA, human replication protein A; hSSB1, human single-stranded DNA binding protein 1; nt, nucleotide(s); PMSF, phenylmethanesulfonyl fluoride; PNK, polynucleotide kinase; ss, single-stranded; SSB, single-stranded DNA binding; TBE 1×, 90 mM Tris, 90 mM borate, and 2 mM EDTA; TE, 10 mM Tris-HCl (pH 7.8) and 1 mM EDTA; TEV, tobacco etch virus; TNR, trinucleotide repeats; WT, wild-type.

 Published on Web 12/29/2010

Humans carry two homologues of p32, RPA2 and RPA4, each of which can assemble with the p70 and p14 subunits to constitute two different RPA complexes (*26*). Recent studies on the alternative RPA, aRPA, composed of p70, RPA4, and p14 suggest a role for aRPA in DNA repair (*27*−*30*). As a consequence of these differences in quaternary structure organization, the length of the ss DNA occluded by SSB proteins can range from 7 nt for T4 SSB protein to 65 nt for the *E. coli* SSB protein octamer. However, SSB proteins can bind shorter ss DNAs [e.g., 3−4 nt for T4 SSB protein (*31*), 8 nt for *E. coli* SSB protein (*32*), and 8−10 nt for hRPA (*33*)].

If the thermodynamics and kinetics of the binding of SSB proteins to nonspecific ss DNA have been extensively studied using long ss or ds lattices, little is known about the functions of specific binding sites, such as ss DNA ends or ds−ss junctions, that can be carried within the DNA substrate of the SSB protein and that can potentially modify the binding properties of the enzyme. For example, a ss gap within a duplex DNA exposes on each side of the gap specific 5′ and 3′ extremities. It has been reported that hRPA assembles in a polar manner on such ss gaps and that p70 mainly interacts with the 5′ end of the downstream primer (*34*, *35*). Recognition of the 3′ end of the upstream primer by the p70 or p32 subunit of hRPA depends on the size of the gap (*35*, *36*). Similarly, a helicase moving across ds DNA exposes two ss DNA strands of opposite polarity. Jose et al. recently described the structural specificities of miniforks and ds−ss junctions and speculated about their functional role (*37*).

In 2008, we proposed a new model for replication-mediated deletions of trinucleotide repeats (TNR) in which SSB protein activity at the replication fork is critical (*38*). In this model, the TNR sequence that the replisome must replicate induces a greater impediment for the leading than for the lagging DNA polymerase and creates transient uncoupling between the replicative helicase and the leading DNA polymerase. To save time for DNA synthesis and restore its coupling with the moving helicase, the leading DNA polymerase passes over a small track of naked leading ss template. By this mechanism, polymerase−helicase coupling is maintained but at the expense of a hairpin that is formed on the template strand after protein coupling has been re-established. Inherent in this model is the requirement for the SSB protein not to bind the short gap of ss DNA between the helicase and leading DNA polymerase during the protein uncoupling phase. This can be accomplished in two ways: either protein coupling is restored before an SSB protein binding site is exposed on the leading template, or SSB protein binds weakly to the leading ss template.

As a first step in dissecting this new model, we have investigated whether leading and lagging ss templates were covered by SSB proteins with equal efficiency. The binding of a variety of SSB proteins to model miniforks exposing a 3′ leading or a 5′ lagging ss DNA arm was characterized. This study was extended to ds−ss junctions with 5′ or 3′ ss tails because such junctions are intermediate structures during gap or ds break repair. Our results show that T4 SSB protein, *E. coli* SSB protein, and hRPA have different binding preferences for ss tails exposed on model miniforks and ds−ss junctions. T4 SSB protein preferentially binds substrates with 5′ ss tails, whereas *E. coli* SSB protein and hRPA prefer substrates with 3′ ss DNA overhangs. Binding preference does not require cooperative binding. hSSB1 exhibits no preferential binding. The nature of the molecular species assembled on miniforks was identified. Surprisingly, we discovered that all the SSB proteins tested not only bind the daughter ss arm of the minifork but also invade and destabilize its daughter ds arm. T4 SSB protein displays this unwinding activity in a polar manner. Unwinding of the ds part of the ds−ss junction is also observed for all SSB proteins studied. These results are discussed in terms of a potential role of the SSB protein in the reversal of a stalled replication fork and in the gap repair-mediated expansion of repetitive sequences.

EXPERIMENTAL PROCEDURES

Enzymes. T4 polynucleotide kinase (PNK) was from New England Biolabs; *E. coli* SSB protein was from USB. Wild-type (WT) and mutant gp32leu106 T4 SSB proteins were overexpressed and purified as described previously (*39*), and their concentrations were measured by UV spectroscopy using extinction coefficients of 39420 and 38000 M^{-1} cm^{-1} for WT and mutant T4 SSB protein, respectively. hRPA was a gift from U. Hübscher (University of Zurich, Zurich, Switzerland) and M. Wold (University of Iowa, Iowa City, IA). His-tagged tobacco etch virus (TEV) protease was prepared as recommended previously (*40*). The plasmid overexpressing His-tagged hSSB1 was a gift from M. F. White (University of St Andrews, St Andrews, U.K.) and was used to subclone the hSSB1 gene into the pSKB3 vector [a gift from S. K. Burley (Lilly Biotechnology Center, San Diego, CA)] to allow the purification of an untagged hSSB1 protein after cleavage of its His tag by the His-tagged TEV protease. BL21-DE3 was used to overexpress hSSB1, and transformed cells were grown in LB with kanamycin (30 μg/mL) at 37 °C while being shaken (180 rpm). To induce protein overexpression, isopropyl β-D-thiogalactoside (IPTG) was added to a final concentration of 0.4 mM when the cell culture had reached an OD_{600} of 0.5. Cells were harvested 4 h after induction of protein expression. To purify hSSB1, 3.6 g of cell paste was first lysed in 50 mL of buffer A [50 mM sodium phosphate (pH 8), 300 mM NaCl, 10 mM imidazole, and 2 mM β-mercaptoethanol] supplemented with 0.75 mg/mL phenylmethanesulfonyl fluoride (PMSF) and 1 mg/mL lysozyme for 40 min on ice under gentle stirring. The cell suspension was then sonicated to reach an OD_{660} of 0.7 and clarified by centrifugation (1.5 h at 4 °C and 117524*g*). The clear crude extract was applied to a 1 mL Ni-NTA (Qiagen) column pre-equilibrated with buffer A at a flow rate of 0.5 mL/min. The column was washed with 10 mL of buffer A, and the protein was eluted by steps of increasing imidazole concentration (10 mL of buffer A with 20 mM imidazole, 10 mL of buffer A with 50 mM imidazole, 10 mL of buffer A with 110 mM imidazole, and 20 mL of buffer A with 230 mM imidazole). Fractions (1 mL) were collected and analyzed by sodium dodecyl sulfate−polyacrylamide gel electrophoresis. The hSSB1-containing fractions were dialyzed against 2 L of buffer B [50 mM sodium phosphate (pH 8), 100 mM NaCl, and 2 mM β-mercaptoethanol] for 12 h. After dialysis, hSSB1 was digested with the His-tagged TEV protease (protease added in a 1:20 mass ratio) for 24 h at 4 °C under gentle shaking. After digestion, NaCl was added to the digestion mix to a final concentration of 300 mM, and the mix was loaded onto a 1 mL Ni-NTA column pre-equilibrated in buffer A. The column was washed with 10 mL of buffer A. Untagged hSSB1 was found in the column flow-through and in the first few fractions of the column wash. The protein was dialyzed againt 2 L of buffer C [20 mM Tris-HCl (pH 8), 30 mM imidazole, and 1 mM dithiothreitol (DTT)] for 12 h and applied to a 1.5 mL heparin (IBF Biotechnics) column pre-equilibrated with buffer C at a flow rate of 0.7 mL/min. The

Table 1: Names and Sequences of Oligonucleotides

name	sequence
H30	5′-TGGCGGCCGCTCGAGCATGCATCTAGAGAGGG-3′
H30c	5′-CCCTCTAGATGCATGCTCGAGCGGCCGCCA-3′
Ta30c	5′-CAACTCACCTGTTTAGCTATATTTTCATTT-3′
Tb30c	5′-TATGTTTCGTAATTCCTTTTGAGGTAATTC-3′
H30(T)9	5′-TGGCGGCCGCTCGAGCATGCATCTAGAGGGTTTTTTTTT-3′
(T)9H30c	5′-TTTTTTTTTCCCTCTAGATGCATGCTCGAGCGGCCGCCA-3′
H30Tal8	5′-TGGCGGCCGCTCGAGCATGCATCTAGAGGCTCGAAGCACAGGTGAGTTG-3′
Tb18H30c	5′-GAACCGAAGGAACGAAACCCCTCTAGATGCATGCTCGAGCGGCCGCCA-3′
H30(AAC)6	5′-TGGCGGCCGCTCGAGCATGCATCTAGAGGGAACAACAACAACAACAAC-3′
(AAC)6H30c	5′-AACAACAACAACAACAACCCCTCTAGATGCATGCTCGAGCGGCCGCCA-3′
H30(CTG)6	5′-TGGCGGCCGCTCGAGCATGCATCTAGAGGGAACAACAACAACAACAAC-3′
(CAG)6H30c	5′-CAGCAGCAGCAGCAGCAGCCCTCTAGATGCATGCTCGAGCGGCCGCCA-3′
H30(CTG)6	5′-TGGCGGCCGCTCGAGCATGCATCTAGAGGGCTGCTGCTGCTGCTGCTG-3′
(CTG)6H30c	5′-CTGCTGCTGCTGCTGCTGCCCTCTAGATGCATGCTCGAGCGGCCGCCA-3′
H30Ta30	5′-TGGCGGCCGCTCGAGCATGCATCTAGAGGGAAATGAAAATATAGCTAAACAGGTGAGTTG-3′
Tb30H30c	5′-GAATTACCTCAAAAGGAATTACGAAACATACCCTCTAGATGCATGCTCGAGCGGCCGCCA-3′
H70	5′-ATAGGGAGACCCAAGCTAATTCTGCAGATATCCATCACACTGGCGGCCGCTC GAGCATGCATCTAGAGGG-3′
H70c	5′-CCCTCTAGATGCATGCTCGAGCGGCCGCCAGTGTGATGGATATCTGCAGAATTA GCTTGGGTCTCCCTAT-3′
H70Ta30	5′-ATAGGGAGACCCAAGCTAATTCTGCAGATATCCATCACACTGGCGGCCGCTCGAGCATGCATC TAGAGGGAAATGAAAATATAGCTAAACAGGTGAGTTG-3′
Tb30H70c	5′-GAATTACCTCAAAAGGAATTACGAAACATACCCTCTAGATGCATGCTCGAGCGGCCG CCAGTGTGATGGATATCTGCAGAATTAGCTTGGGTCTCCCTAT-3′

column was next washed with 15 mL of buffer C, and the protein was eluted with a 40 mL salt gradient (from 0 to 1 M NaCl). Fractions (3 mL) were collected and analyzed by sodium dodecyl sulfate−polyacrylamide gel electrophoresis. hSSB1-containing fractions were dialyzed against 1 L of prestorage buffer [20 mM sodium phosphate (pH 7.5), 50 mM NaCl, 1 mM DTT, and 25% glycerol] for 12 h and against 1 L of storage buffer [20 mM sodium phosphate (pH 7.5), 50 mM NaCl, 1 mM DTT, and 50% glycerol] for 8 h. The protein was estimated to be at least 90% pure by Coomassie Blue staining. Its concentration was measured by UV spectroscopy using an extinction coefficient of 11500 M^{-1} cm^{-1}.

Oligonucleotide Sequences. The sequences of the oligonucleotides (Eurogentec) used here are listed in Table 1. All oligonucleotides were gel purified before use. DNA concentrations were determined by UV spectroscopy using the extinction coefficients provided by the manufacturer.

Radiolabeling of Oligonucleotides. Radiolabeling of oligonucleotides at their 5′ extremity was performed by incubating 1 μM oligonucleotide with 1 μM [γ-^{32}P]ATP, 1 μM ATP, and PNK (0.2 unit/mL) in PNK 1× buffer for 45 min at 37 °C. Nonincorporated [γ-^{32}P]ATP and ATP were removed using a Biospin 6 column (Bio-Rad) equilibrated in TE buffer.

Preparation of ds−ss Junctions and Miniforks. ds−ss junctions and miniforks contain a single 5′ ^{32}P-labeled oligonucleotide, which is indicated in each figure by an asterisk. ds−ss junctions were prepared by mixing the radiolabeled oligonucleotide with its partially complementary strand in a 1:4 molar ratio. Miniforks were prepared by mixing three oligonucleotides. The two nonradiolabeled strands were added in a 4-fold molar excess relative to the radiolabeled strand. A 4-fold excess of complementary unlabeled strands was used to keep the two strands of the ds−ss junctions or the three strands of the miniforks well annealed. Strand hybridization was performed by heating (5 min at 95 °C) and slow cooling. Hybridization was checked by electrophoresis on a native polyacrylamide gel (10% acrylamide and 7% acrylamide for ds−ss junctions and miniforks, respectively). The mass ratio of acrylamide and bisacrylamide was 29:1, and native gels were made in TBE 1×. A major conformation representing at least 75% of the total material was observed for most DNA substrates. DNA substrates used for T4 SSB protein and *E. coli* SSB protein interactions were prepared in a buffer consisting of 40 mM Tris-HCl (pH 7.5), 50 mM NaCl, and 20 mM $MgCl_2$. DNA substrates used for hRPA interaction were prepared in a buffer consisting of 30 mM HEPES (pH 7.8), 50 mM NaCl, and 7 mM $MgCl_2$. DNA substrates used for interactions with hSSB1 were prepared in a buffer consisting of 20 mM HEPES (pH 7.8), 75 mM NaCl, and 20 mM EDTA.

Band-Shift Assays. Interactions between SSB proteins and DNA were performed in the buffer used to prepare the DNA substrates supplemented with 2 mM DTT. The proteins at increasing concentrations (indicated in each figure) were incubated with 25 nM radiolabeled DNA (with 75 nM unlabeled DNA) for 10 min at 22 °C, except for the 30−70 junctions for which incubation took place at 4 °C. Samples were then loaded on a native polyacrylamide gel to resolve the different molecular species. The level of acrylamide ranged from 10% (for the 30−9 junctions) to 6% (for miniforks), and the mass ratio of acrylamide to bisacrylamide was 29:1. Native gels were prepared in TBE 1×. Electrophoresis was performed at 4 °C and 30 mA for 2.5 h. After electrophoresis, the gel was dried and exposed on a phosphorimager screen. After being exposed for at least 10 h, the screen was scanned with a Storm 820. The samples in the gel were quantified using ImageQuant version 5.1 or NT. Each experiment was reproduced at least twice. When indicated, error bars correspond to the standard deviation calculated from at least two independent experiments. To estimate the difference in binding between miniforks with a 5′ or 3′ daughter ss tail, DNA substrates were tested in parallel with the same freshly diluted enzymes. Similarly, ds−ss DNA junctions with opposite ss tail polarity were tested in parallel with the same freshly diluted protein stocks.

Table 2: Substrates

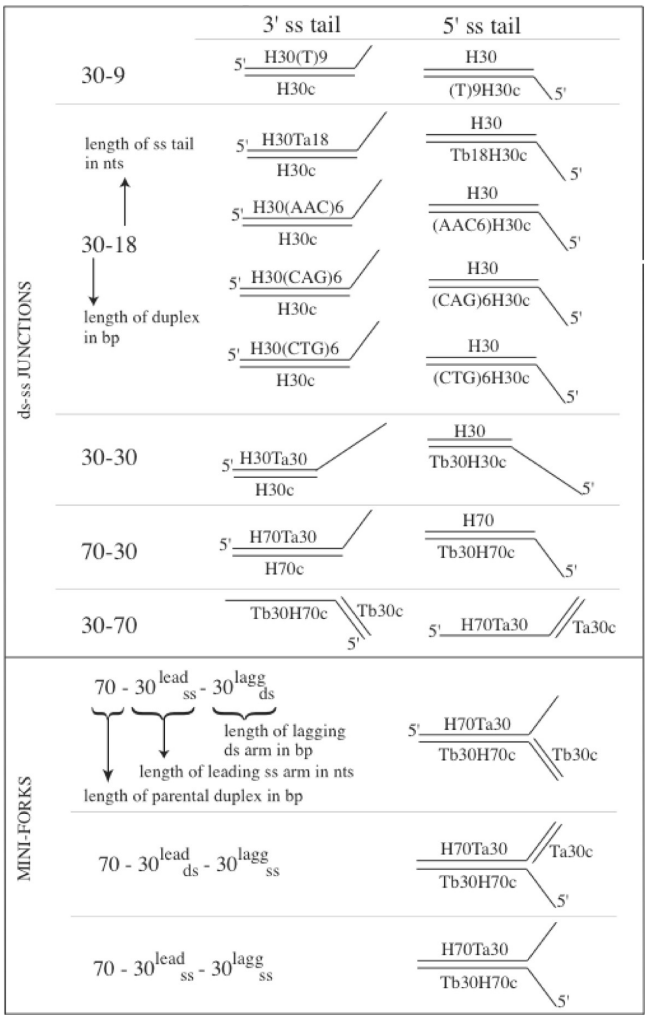

RESULTS

Nomenclature. The sequences of the oligonucleotides used in this study are listed in Table 1. ds−ss junctions (Table 2) are designated by two numbers: the first and second numbers that are separated by a dash specify the length of the ds and ss parts of the junction, respectively. The lengths of the ds and ss parts of the junction are given in base pairs and nucleotides. For example, the 30−18 junctions (Table 2) consist of a 30 bp duplex carrying an 18 nt ss tail and are made by annealing a 48-mer with a 30-mer. The different 30−18 junctions represented in Table 2 differ by the orientation (3′ or 5′) and the sequence (random sequence, AAC, CAG, or CTG repeats) of the ss tail. Model miniforks (Table 2) consist of a parental duplex and two daughter arms (leading and lagging), which can be ss or ds. The designation "leading" or "lagging" for minifork daughter arms originates from the terminology used in DNA replication. A daughter arm is named leading if the template strand exposed by the helicase has a 3′ extremity. Similarly, a daughter arm is named lagging if the template strand exposed by the helicase has a 5′ extremity. Miniforks are designated by three numbers that are separated by dashes and that refer to the length of the parental duplex (first number) and the length of both daughter arms (second and third numbers). Adjacent to the length of the arm, the type of daughter arm (lead vs lagg) and its nature (ss vs ds) are indicated in superscript and subscript, respectively. For example, the minifork designated 70−30^{lead}_{ss}−30^{lagg}_{ds} (Table 2) consists of a 70 bp parental duplex with a 30 nt leading ss arm and a 30 bp lagging ds arm.

T4 SSB Protein, E. coli SSB Protein, and hRPA Have Different Preferential Binding Polarities on Model Miniforks, whereas hSSB1 Does Not Exhibit Any Preferential Binding. Once loaded at the replication fork, the helicase unwinds the parental ds DNA and exposes daughter ss templates of opposite polarity. T4 SSB protein has been reported to bind with higher affinity to DNA miniforks with a 5′ ss arm than to DNA miniforks with a 3′ ss arm (*41*), suggesting that the lagging ss template is more efficiently covered by T4 SSB proteins than the leading ss template. To investigate whether this property is shared by other SSB proteins and is conserved among species, we constructed miniforks with either a 5′ or 3′ ss tail and characterized the binding properties of *E. coli* SSB protein, hRPA, and hSSB1.

To first test our DNA substrates, we investigated the binding of T4 SSB protein with 70−30^{lead}_{ss}−30^{lagg}_{ds} and 70−30^{lead}_{ds}−30^{lagg}_{ss} miniforks by titrating the protein with 5′ radiolabeled DNA substrates and resolving the species by electrophoresis on a native gel (Figure 1A). As the protein concentration increases, DNA is trapped into nucleoprotein complexes with lower mobilities than naked DNA. The smeary appearance of the bands is possibly due to the low intrinsic affinity of T4 SSB proteins for ss DNA and the small number (four) of binding sites of T4 SSB protein on the ss tail of the miniforks. Protein−DNA complexes can dissociate during electrophoresis. Qualitative inspection of the retardation gel indicates that binding is more cooperative on the 70−30^{lead}_{ds}−30^{lagg}_{ss} substrate than on the 70−30^{lead}_{ss}−30^{lagg}_{ds} minifork because a stable protein−DNA complex with its ss tail fully covered by T4 SSB protein [species indicated by two asterisks (Figure 1A)] forms and accumulates at lower protein concentrations with the 70−30^{lead}_{ds}−30^{lagg}_{ss} substrate than with the 70−30^{lead}_{ss}−30^{lagg}_{ds} substrate (in Figure 1A, compare lanes 15−17 and lanes 23−25). Retardation gels were quantified by measuring the proportion of protein−DNA complexes as a function of protein concentration. The affinity difference between the two forks is best observed at midtitration (0.675 μM T4 SSB protein, lanes 15 and 23, Figure 1A) where the proportion of protein−DNA complexes equals 70 and 56% for 70−30^{lead}_{ds}−30^{lagg}_{ss} and 70−30^{lead}_{ss}−30^{lagg}_{ds} miniforks, respectively. The mean ratio (R) between the percentage of protein−DNA complexes formed with 70−30^{lead}_{ds}−30^{lagg}_{ss} and that formed with 70−30^{lead}_{ss}−30^{lagg}_{ds} equals 1.65 ± 0.5 (right panel, Figure 1B). The binding property of T4 SSB protein was also investigated on miniforks carrying a 30 bp parental duplex and daughter arms of 30 nt and 30 bp [30−30−30 miniforks (Figure 1B)]. A similar value of R [1.62 ± 0.4 (right panel, Figure 1B)] was measured with these miniforks, confirming the preference of the T4 SSB protein for miniforks carrying a lagging ss tail. On the whole, our quantitative analysis of the retardation gels confirms the results of Jones et al. (*41*) and validates the use of our miniforks under the experimental conditions used here.

As opposed to those with T4 SSB protein, band-shift experiments performed with *E. coli* SSB protein and hRPA show a binding preference for miniforks carrying a leading ss strand (Figure 1C,D). Experiments performed with hSSB1 indicate that this protein does not exhibit any preference for a minifork ss tail (data not shown).

T4 SSB Protein, E. coli SSB Protein, and hRPA Can Unwind the Newly Synthesized ds Arm of a Minifork. Several protein−DNA complexes with different electrophoretic mobilities on retardation gels are formed when miniforks are

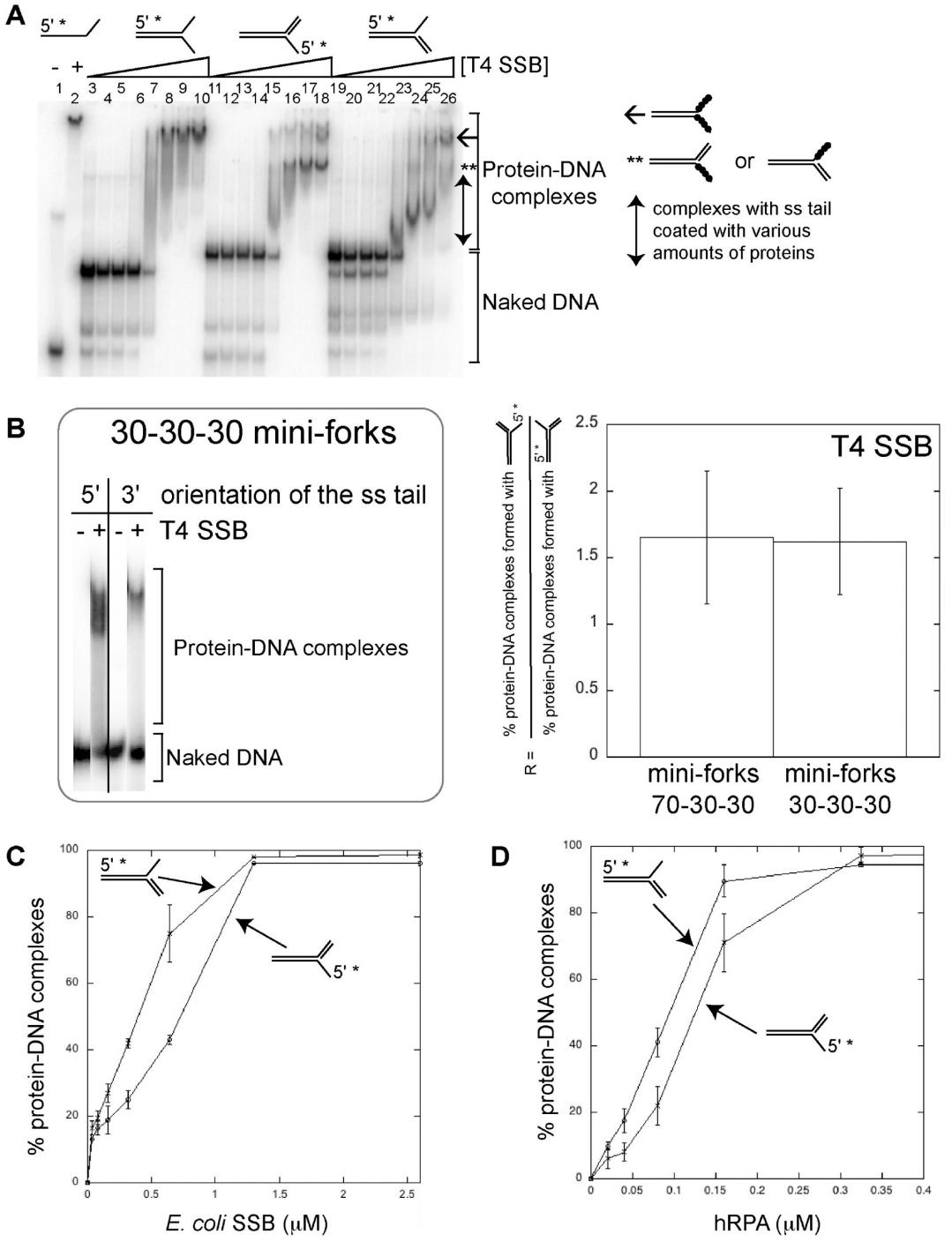

FIGURE 1: T4 SSB protein, *E. coli* SSB protein, and hRPA bind the ss tails of miniforks with polarity. Interactions between proteins and DNA were assessed and native gel electrophoresis performed as described in Experimental Procedures. Protein concentrations are given in monomeric units for T4 SSB protein, homotetrameric units for *E. coli* SSB protein, and heterotrimeric units (p70−p32−p14) for hRPA. Error bars correspond to the standard deviation calculated from at least two independent experiments. (A) The radiolabeled strand of each substrate is denoted with an asterisk. Except for H70Ta30 for which interaction with T4 SSB protein is assessed at 5.4 μM (lane 2), the T4 SSB protein concentration (given in micromolar) increases as follows: 0 (lanes 1, 3, 11, and 19), 0.0835 (lanes 4, 12, and 20), 0.17 (lanes 5, 13, and 21), 0.34 (lanes 6, 14, and 22), 0.675 (lanes 7, 15, and 23), 1.35 (lanes 8, 16, and 24), 2.7 (lanes 9, 17, and 25), and 5.4 (lanes 10, 18, and 26). The protein−DNA complex specific for $70{-}30^{lead}{}_{ss}{-}30^{lagg}{}_{ss}$ with both daughter ss tails fully covered by T4 SSB protein is denoted with a backward arrow. The protein−DNA complex specific for $70{-}30^{lead}{}_{ss}{-}30^{lagg}{}_{ds}$ and $70{-}30^{lead}{}_{ds}{-}30^{lagg}{}_{ss}$ with its daughter ss tail fully covered by T4 SSB protein is denoted with two asterisks. Nucleoprotein complexes with their daughter ss tails coated with various amounts of protein are denoted with a double-headed arrow. (B) Interaction of T4 SSB protein with $30{-}30^{lead}{}_{ss}{-}30^{lagg}{}_{ds}$ (3′ orientation of the ss tail) and $30{-}30^{lead}{}_{ds}{-}30^{lagg}{}_{ss}$ (5′ orientation of the ss tail) at 0.675 μM protein (left). The ratio R between the percentage of protein−DNA complexes formed at 0.675 μM protein with miniforks containing a 5′ daughter ss tail and that formed with miniforks containing a 3′ daughter ss tail has been calculated for 70−30−30 and 30−30−30 miniforks (right). (C) Percentage of *E. coli* SSB protein in a complex with 70−30−30 miniforks as a function of protein concentration. (D) Percentage of hRPA in a complex with 70−30−30 miniforks as a function of protein concentration.

titrated with proteins. To identify more precisely the nature of the nucleoprotein complex present in each retarded band, miniforks radiolabeled at the 5′ end of the 100-mer were prepared. Protein titrations were performed with $70{-}30^{lead}{}_{ss}{-}30^{lagg}{}_{ds}$ and

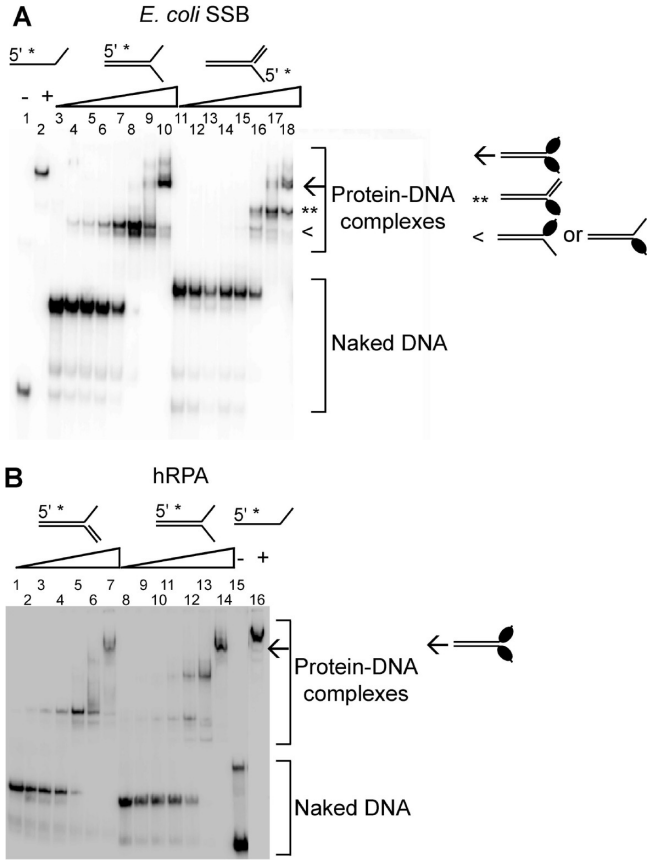

FIGURE 2: Nucleoprotein complex with both daughter ss tails covered by SSB protein that accumulates as the *E. coli* SSB protein or hRPA concentration increases. The miniforks consist of a 70 bp parental DNA and daughter arms of 30 bp and 30 nt. The radiolabeled strand of each substrate is denoted with an asterisk. The protein−DNA complex specific for the $70-30^{lead}{}_{ss}-30^{lagg}{}_{ss}$ minifork with both daughter ss tails covered by *E. coli* SSB protein (A) or hRPA (B) is denoted with a backward arrow. (A) Except for H70Ta30 for which interaction with *E. coli* SSB protein is assessed at 2.6 μM (lane 2), the *E. coli* SSB protein concentration (given in micromolar) increases as follows: 0 (lanes 1, 3, and 11), 0.04 (lanes 4 and 12), 0.08 (lanes 5 and 13), 0.16 (lanes 6 and 14), 0.325 (lanes 7 and 15), 0.65 (lanes 8 and 16), 1.3 (lanes 9 and 17), and 2.6 (lanes 10 and 18). The protein−DNA complex specific for the $70-30^{lead}{}_{ss}-30^{lagg}{}_{ss}$ minifork with one of its daughter ss tails covered by *E. coli* SSB protein is denoted by <. The protein−DNA complex specific for the $70-30^{lead}{}_{ss}-30^{lagg}{}_{ds}$ minifork and for the $70-30^{lead}{}_{ds}-30^{lagg}{}_{ss}$ minifork with its daughter ss tail covered by *E. coli* SSB protein is denoted with two asterisks. (B) The hRPA concentration (given in micromolar) increases as follows: 0 (lanes 1, 8, and 15), 0.02 (lanes 2 and 9), 0.04 (lanes 3 and 10), 0.08 (lanes 4 and 11), 0.16 (lanes 5 and 12), 0.325 (lanes 6 and 13), and 0.65 (lanes 7, 14, and 16).

$70-30^{lead}{}_{ds}-30^{lagg}{}_{ss}$ miniforks, the $70-30^{lead}{}_{ss}-30^{lagg}{}_{ss}$ substrate, and the ss radiolabeled 100-mer that is used to prepare the miniforks. Electrophoretic migration profiles were then compared. Surprisingly, one of the nucleoprotein complexes that accumulates at the end of the titration with the T4 SSB and *E. coli* SSB proteins has the same mobility as the $70-30^{lead}{}_{ss}-30^{lagg}{}_{ss}$ substrate covered by the SSB protein (species denoted with backward arrows in Figures 1A and 2A; in Figure 1A, compare lanes 10, 18, and 26; in Figure 2A, compare lanes 10 and 18). The same applies to hRPA (species denoted with a backward arrow in Figure 2B; compare lanes 7 and 14). The electrophoretic migration of this species is different from that of the 100-mer when tested at the same protein concentration (in Figure 1A, compare lanes 2, 10, 18, and 26; in Figure 2A, compare lanes 2, 10, and 18; in Figure 2B, compare lanes 7, 14, and 16). This result suggests that after binding the daughter ss arm of the minifork, T4 SSB protein, *E. coli* SSB protein, and hRPA can invade and unwind the opposite daughter ds arm of the minifork. To confirm these results, we constructed $70-30^{lead}{}_{ss}-30^{lagg}{}_{ds}$ and $70-30^{lead}{}_{ds}-30^{lagg}{}_{ss}$ miniforks radiolabeled on the 5′ end of the 30-mer. If the SSB proteins were able to destabilize the daughter ds arm after binding the daughter ss arm of the minifork, then a species corresponding to a 30-mer covered by SSB protein should form and accumulate during protein titration. Band-shift experiments performed with these miniforks, the 5′ radiolabeled 30-mer, and all three SSB proteins show the accumulation of a species that has the same mobility as a 30-mer covered by SSB protein (species denoted with a backward arrow in Figure 3A−C). This result confirms that T4 SSB protein, *E. coli* SSB protein, and hRPA can unwind the daughter ds arm of the minifork. Destabilization of the newly synthesized daughter arm of the miniforks starts to take place once the daughter ss tail of the miniforks is covered and when the protein is in a 2−5-fold molar excess [1.35 μM T4 SSB protein (lanes 16 and 24, Figure 1A), 1.3 μM *E. coli* SSB protein (lane 17, Figure 2A), and 0.65 μM hRPA (lane 7, Figure 2B)]. For T4 SSB protein, the efficiency of this duplex destabilization reaction is substrate specific. Indeed, the percentage of T4 SSB protein in a complex with the labeled 30-mer at the end of protein titration (% 30−SSB in Figure 3A) indicates that T4 SSB protein unwinds the ds daughter lagging arm of the $70-30^{lead}{}_{ss}-30^{lagg}{}_{ds}$ minifork more efficiently than the ds daughter leading arm of the $70-30^{lead}{}_{ds}-30^{lagg}{}_{ss}$ minifork. The mean ratio of the percentage of T4 SSB protein in a complex with the labeled 30-mer of the $70-30^{lead}{}_{ss}-30^{lagg}{}_{ds}$ minifork to that of the $70-30^{lead}{}_{ds}-30^{lagg}{}_{ss}$ minifork equals 2.5 ± 0.5. Because the 30 bp duplexes of each minifork have the same melting temperature, this result suggests polar duplex destabilization, with a preference for miniforks containing a 3′ ss leading tail. On the other hand, *E. coli* SSB protein unwinds both miniforks with comparable efficiency (% 30−SSB in Figure 3B). The mean ratio of the percentage of *E. coli* SSB protein in a complex with the labeled 30-mer of the $70-30^{lead}{}_{ss}-30^{lagg}{}_{ds}$ minifork to that of the $70-30^{lead}{}_{ds}-30^{lagg}{}_{ss}$ minifork equals 1.4 ± 0.2.

hRPA, T4 SSB Protein, and E. coli SSB Protein Have Different Preferential Binding Polarities on ds−ss Junctions, whereas hSSB1 Exhibits No Preferential Binding. The model miniforks used here are asymmetric in the sense that exposed ss DNAs have opposite polarities. DNA forms with ss overhangs are also asymmetric structures depending on the polarity of the ss overhang. Two independent studies investigated the binding polarity of hRPA on ss DNA using asymmetric structures consisting of ds DNA with 5′ or 3′ ss overhangs but reached opposite conclusions (*34*, *42*). To further examine these conflicting data and investigate whether other SSB proteins have a binding preference for a ss tail with a defined polarity, a variety of ds−ss junctions with either a 5′ or 3′ ss tail were prepared and the binding properties of T4 SSB protein, hRPA, *E. coli* SSB protein, and hSSB1 were characterized by band-shift assays.

Figure 4A shows the quantitative analysis of titration of WT T4 SSB protein with 30−9 ds−ss junctions carrying either a 5′ or a 3′ 9 nt ss tail. The sequence of the ss tail consists of a repetition of nine T residues. With the knowledge that the T4 SSB protein binding site is 6−7 nt in length (*9*), the 30−9 junction allows the binding of only one T4 SSB protein per substrate, making it possible to investigate whether cooperativity is required for preferential binding. The results indicate that the WT T4 SSB

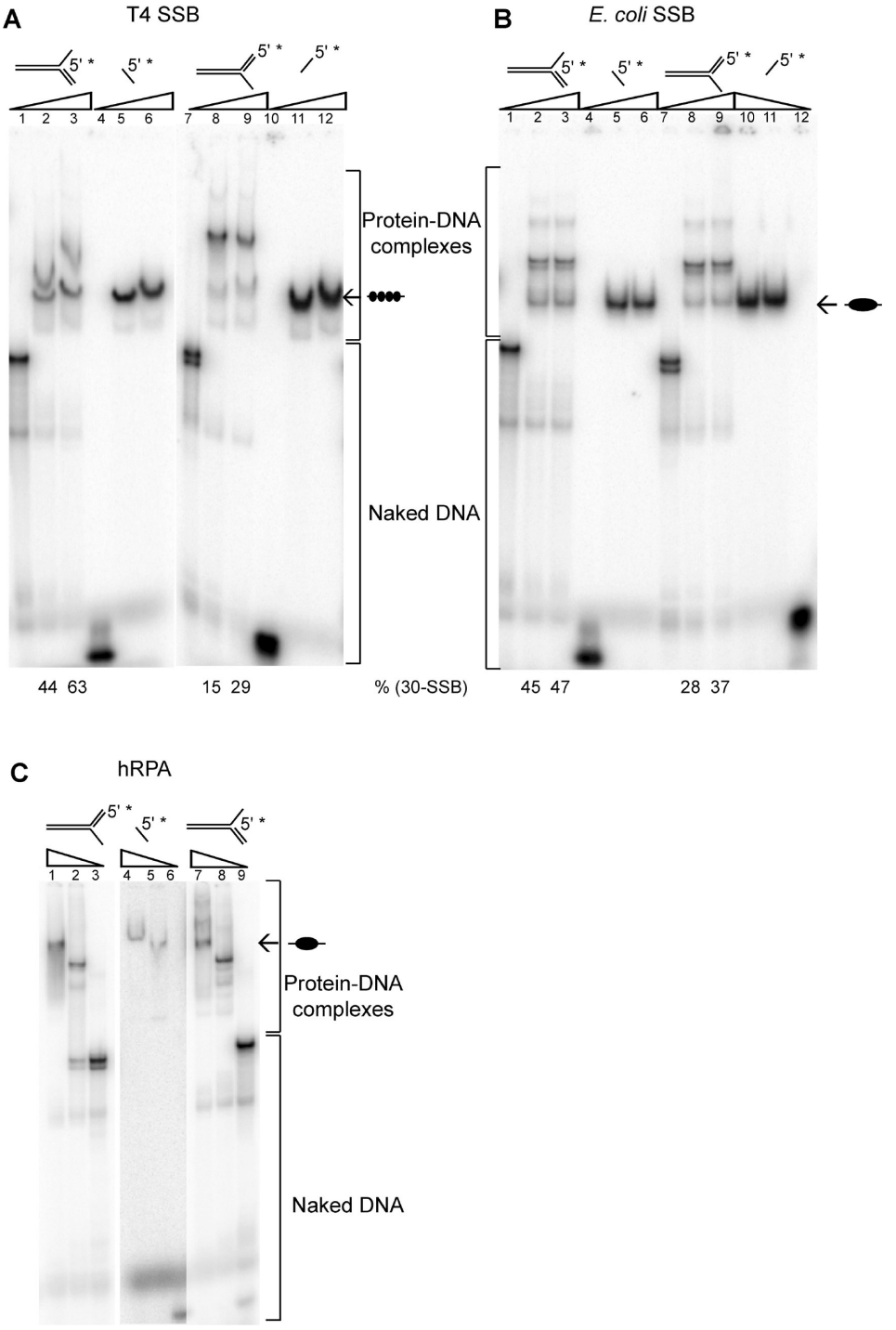

FIGURE 3: T4 SSB protein, *E. coli* SSB protein, and hRPA can unwind the newly synthesized daughter ds DNA of miniforks. Miniforks are labeled on the Ta30c or Tb30c 30-mers as indicated. The protein−DNA complex formed with the radiolabeled 30-mer is denoted with a backward arrow. (A) The three T4 SSB protein concentrations (given in micromolar) tested were 0 (lanes 1, 4, 7, and 10), 4.5 (lanes 2, 5, 8, and 11), and 13.5 (lanes 3, 6, 9, and 12). The percentage of 30-mer in a complex with T4 SSB protein (% 30−SSB) at each protein concentration tested (4.5 and 13.5 μM) is given for the $70-30^{lead}{}_{ss}-30^{lagg}{}_{ds}$ (lanes 2 and 3) and $70-30^{lead}{}_{ds}-30^{lagg}{}_{ss}$ (lanes 8 and 9) miniforks. (B) The three *E. coli* SSB protein concentrations (given in micromolar) tested were 0 (lanes 1, 4, 7, and 12), 2 (lanes 2, 5, 8, and 11), and 6.5 (lanes 3, 6, 9, and 10). (C) The three hRPA concentrations (given in micromolar) tested were 0 (lanes 3, 6, and 9), 0.3 (lanes 2, 5, and 8), and 1 (lanes 1, 4, and 7).

protein prefers binding to a ds−ss junction with a 5′ ss tail. The preference for ds−ss junctions with a 5′ ss tail is consistent with the T4 SSB protein preference for miniforks containing a 5′ lagging ss arm (Figure 1A,B). Furthermore, our result indicates that the preferential binding of T4 SSB protein on ds−ss junctions with a 5′ ss tail does not rely on cooperativity. To further validate this result for cooperativity, the binding property of a T4 SSB protein mutant, gp32leu106, was also characterized. This mutant binds ss DNA with a lower affinity than WT T4 SSB protein because of a lower intrinsic affinity for ss DNA and a lower cooperativity factor (intrinsic affinity of 1.8×10^5 M^{-1}, cooperativity factor ω of 130) (*43*). Band-shift experiments performed on 30−9 junctions confirm that the gp32leu106 protein has a weaker affinity for ss DNA than the WT T4 SSB protein and show that this mutant protein still prefers binding to a ds−ss junction with a 5′ ss tail (Figure 4A). Therefore,

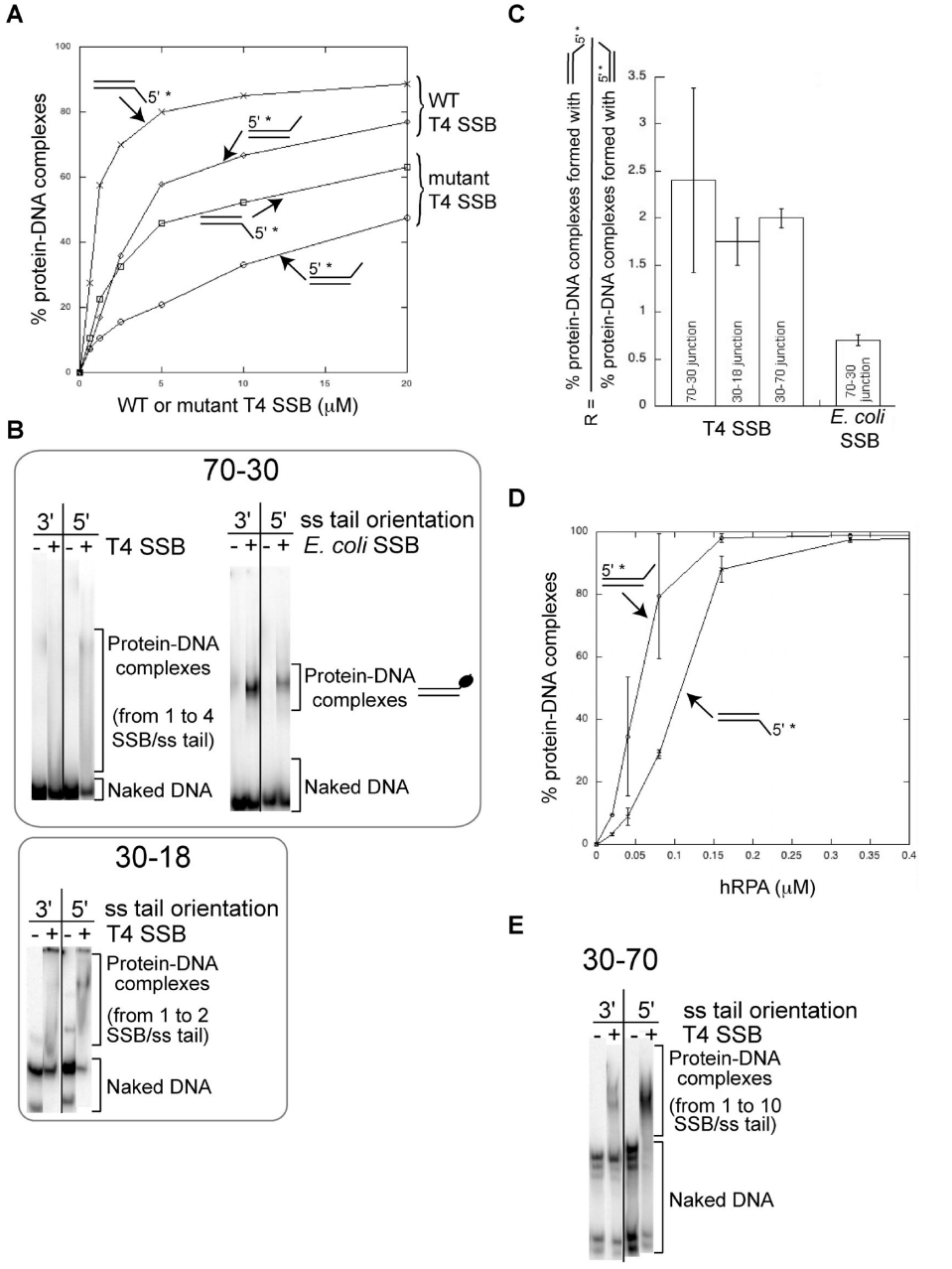

FIGURE 4: T4 SSB, hRPA, and *E. coli* SSB proteins bind the ss tail of ds−ss junctions with polarity. Where indicated, error bars correspond to the standard deviation calculated from at least two independent experiments. (A) The graph shows the percentage of protein−DNA complexes formed as a function of protein concentration for WT and gp32leu106 mutant T4 SSB proteins and 30−9 ds−ss junctions. The ss tail of the 30−9 ds−ss junctions used in this titration carries nine T residues. (B) The binding of the T4 and *E. coli* SSB proteins to 70−30 ds−ss junctions (top) and of the T4 SSB protein to 30−18 ds−ss junctions (bottom) with a 3′ or 5′ ss tail has been investigated as described in Experimental Procedures. When they interact with 70−30 junctions, the concentrations of T4 and *E. coli* SSB protein are 0.675 and 0.325 μM, respectively; 0.9 μM T4 SSB protein is used to investigate the interaction with the 30−18 junctions. (C) Ratios (R) of the percentage of protein−DNA complexes formed with ds−ss junctions containing a 5′ ss tail to that formed with ds−ss junctions containing a 3′ ss tail calculated for 70−30, 30−18, and 30−70 miniforks. (D) Percentage of hRPA in a complex with 30−18 ds−ss junctions as a function of protein concentration. The ss tail of the 30−18 ds−ss junctions used in this titration carries a repeat of six AAC repeats. (E) Binding of T4 SSB protein to 30−70 junctions investigated at 0.675 μM and 4 °C. The naked 30−70 junctions display several distinct radiolabeled bands possibly reflecting several conformations.

cooperativity is not required for the preferential binding of T4 SSB protein to ds−ss junctions with a 5′ ss tail.

To confirm the ss tail polarity preference of T4 SSB protein on ds−ss junctions, we investigated the binding of T4 SSB protein to two additional ds−ss junctions, 70−30 and 30−18 junctions, whose ss tail consists of a random sequence (Figure 4B; quantified in Figure 4C). The results confirm the preference of T4 SSB protein for ds−ss junctions with a 5′ ss tail because the mean ratio (R) between the percentage of protein−DNA complexes formed at a specific protein concentration with ds−ss junctions containing a 5′ ss tail and that formed with ds−ss junctions containing a 3′ ss tail is greater than one (Figure 4C). On the other hand, *E. coli* SSB protein prefers ds−ss junctions with a 3′ ss tail (Figure 4B; quantified in Figure 4C), consistent with its preference for miniforks containing a 3′ leading ss arm (Figure 1C). The binding preference of hRPA was examined on 30−18 ds−ss junctions. The sequence of the ss tail consists of six AAC repeats. Quantitative analysis of the retardation gels reveals that hRPA preferentially binds to a junction with a 3′ ss tail (Figure 4D), confirming the results of de Laat et al. (*34*). The same result was

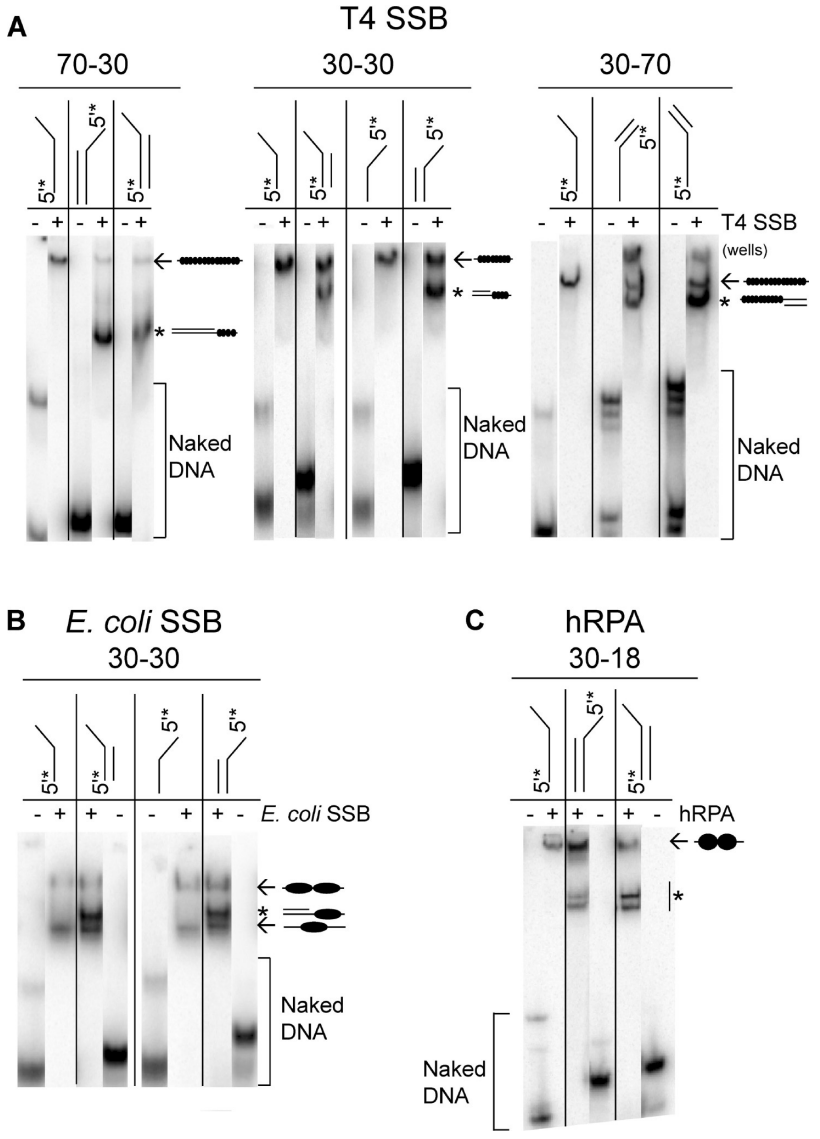

FIGURE 5: T4 SSB protein, *E. coli* SSB protein, and hRPA unwind the ds part of the ds−ss junctions. The radiolabeled strand of each substrate is denoted with an asterisk. The nucleoprotein complex corresponding to the radiolabeled strand fully covered by the SSB protein is denoted with a backward arrow. The nucleoprotein complex corresponding to the ds−ss junction with its ss tail fully covered by the SSB protein is denoted with an asterisk. (A) Interaction between T4 SSB protein and 70−30 (left), 30−30 (middle), and 30−70 (right) junctions investigated at 5.4 μM protein and 22 °C for 70−30 and 30−30 junctions or 4 °C for 30−70 junctions. (B) Interaction between *E. coli* SSB protein and 30−30 junctions investigated at 2.5 μM protein and 22 °C. (C) Interaction between hRPA and 30−18 junctions investigated at 0.65 μM protein and 22 °C. The ss tail of the 30−18 ds−ss junctions carries six AAC repeats. The nucleoprotein complex corresponding to the ds−ss junction with its ss tail fully covered by the SSB protein (denoted with an asterisk) migrates as a doublet possibly reflecting complexes with different stoichiometries as reported in ref *64*.

obtained with 30−18 junctions carrying structure-forming ss tails made of six CAG or CTG repeats (data not shown). The preference for ds−ss junctions with a 3′ ss tail is consistent with the hRPA preference for miniforks containing a 3′ leading ss arm (Figure 1D). Band-shift experiments performed with hSSB1 on ds−ss junctions indicate that as opposed to hRPA, *E. coli* SSB protein, and T4 SSB protein, hSSB1 does not exhibit any preferential binding to ds−ss junctions with opposite ss tail polarities (data not shown).

The Preferential Binding of T4 SSB Protein to ds−ss Junctions with a 5′ ss Tail Persists on ds−ss Junctions with a 70 nt ss Tail. ds−ss junctions carry several types of binding sites: nonspecific ds DNA, nonspecific ss DNA, specific ds or ss DNA ends, and the specific ds−ss junction itself. Preferential binding of T4 SSB protein to ds−ss junctions with a 5′ ss tail may stem from a higher affinity of the protein for a specific site than for nonspecific sites present on the substrate. When the length of the ss tail of the ds−ss junction increases, the number of nonspecific binding sites increases but the number of specific sites does not. Therefore, apparent binding differences between nonspecific and specific binding sites might diminish as the tail length of the ds−ss junction increases, and one expects preferential binding of SSB protein to a ds−ss junction with a specific ss tail polarity to exist up to a definite ss tail length. To investigate this aspect, we characterized the binding of T4 SSB protein to 30−70 junctions. Assuming a binding site of 7 nt for T4 SSB protein (*9*), the 30−70 junction carries the unique specific site constituted by the ds−ss junction and 64 nonspecific overlapping binding sites on the ss tail. The result indicates that even with a 70 nt ss tail, T4 SSB protein still prefers binding to the ds−ss junctions with a 5′ ss tail (Figure 4E; quantified in Figure 4C).

T4 SSB Protein and hRPA Destabilize the Duplex Part of ds−ss Junctions in a Polar Manner. Band-shift experiments

Table 3: Percentages of ds−ss Junctions Unwound by Different SSB Proteins

protein	ds−ss junction name	ds−ss junction ss tail orientation	% unwound ds−ss junction
T4 SSB protein	70−30	3′	3.3 ± 2
		5′	2.9 ± 1.5
	30−30	3′	63 ± 5
		5′	39 ± 3
	30−70	3′	55 ± 20
		5′	34 ± 6
E. coli SSB protein	30−30	3′	50 ± 7
		5′	41.5 ± 10.5
hRPA	30−18	3′	14.5 ± 8.5
		5′	56 ± 18

performed on model miniforks with T4 SSB protein revealed that T4 SSB protein can unwind the newly synthesized ds arm of a minifork with a preference for miniforks containing a 3′ leading ss tail and a 5′ lagging ds arm. *E. coli* SSB protein unwinds the newly synthesized ds arm of miniforks without any preference for the specific ss tail orientation. To investigate whether unwinding also occurred on ds−ss junctions, we incubated T4 SSB protein, *E. coli* SSB protein, and hRPA with ds−ss junctions carrying either a 5′ ss tail or a 3′ ss tail, or with the ss 5′ radiolabeled strand that was used to prepare the ds−ss junctions (100-mer for 70−30 and 30−70 junctions, 60-mer for 30−30 junctions, and 48-mer for 30−18 junctions). The species were then resolved on a native polyacrylamide gel, and the electrophoretic migration profiles were compared. A retarded band (denoted with a backward arrow in Figure 5) migrating with the same mobility as a 100-mer covered by T4 SSB protein is clearly visible in the case of the 70−30 and 30−70 junctions (left and right panels, Figure 5A), suggesting that T4 SSB proteins can unwind these ds−ss junctions. The same is true of the 30−30 junctions for which one of the nucleoprotein complexes that forms has the same mobility as a 60-mer covered by T4 SSB protein (middle panel, Figure 5A). Similarly, *E. coli* SSB protein and hRPA display a helix destabilizing activity on the ds−ss junctions tested (Figure 5B,C). To establish whether duplex destabilization occurred in a polar manner, we compared the proportions of unwound ds−ss junctions. The results indicate that T4 SSB protein preferentially destabilizes ds−ss junctions with a 3′ ss tail (Table 3). This is consistent with the polar duplex destabilization observed for this protein on miniforks (Figure 3A). Although tested on a single type of ds−ss junctions (30−18), hRPA exhibits a preference for the unwinding of ds−ss junctions with a 5′ ss tail (Table 3). No clear preference for unwinding of a 30−30 ds−ss junction with a specific ss tail orientation can be established for *E. coli* SSB protein (Table 3). This result is consistent with the conclusion drawn from analyzing the unwinding of the daughter ds arm of miniforks (Figure 3A).

DISCUSSION

We have investigated the binding properties of a variety of SSB proteins on model miniforks and ds−ss junctions as a first step in dissecting the triplet repeat instability model described previously (*38*). Our results show that T4 SSB protein, *E. coli* SSB protein, and hRPA share the following properties: (i) binding preferentially one orientation of the ss tail of a minifork and (ii) destabilizing the opposite daughter DNA duplex (Figures 1−3). Using ds−ss junctions, several SSB proteins have been reported to destabilize DNA duplexes of various lengths (*10*−*15*), and our studies of the interaction of T4 SSB proteins with ds−ss junctions (Figure 5A) confirm the helix destabilizing property of this protein initially observed on poly{d(A-T)} sequences (*9*). The SSB protein filament assembled around the ss DNA of a ds−ss junction may grow when a new SSB protein monomer binds to the last SSB protein monomer at one end of the filament after exposure of a few ss nucleotides by thermal fluctuations. The duplex destabilizing activity reported here on miniforks is different from that previously described because it requires the SSB protein to melt the opposite daughter ds DNA and to nucleate a new SSB protein filament on at least one end of the duplex strands. Natural ds DNA breathing at the fork (*37*, *44*, *45*) possibly increased by the proximity of bound SSB proteins may help expose a minimal stretch of ss DNA (e.g., 3−4 nt for T4 SSB protein and 8−10 nt for hRPA) to permit the invasion of ss DNA by the protein. As coating of the ss tail of the minifork requires concentrations of SSB protein lower than that for duplex destabilization, we propose that covering the newly synthesized DNA precedes daughter ds arm melting. Daughter duplex destabilization leads to the formation of a minifork intermediate on which both leading and lagging templates and one of the newly synthesized DNAs are coated with SSB proteins (Figure 6A). Yeast Rad52 (*46*−*48*), human Rad52 (*49*), *E. coli* RecO (*50*), and bacteriophage T4 UvsY (*50*), the functional homologues of Rad52 in *E. coli* and T4, have been reported to be able to anneal complementary ss DNAs coated by their cognate SSB proteins, and this activity is proposed to allow second-end DNA capture during homologous recombination-mediated ds break repair. The substrate created after SSB protein binding and duplex unwinding of the daughter arm of the minifork is suitable for Rad52/RecO-mediated ss reannealing, which ultimately will promote fork reversal (Figure 6A). Therefore, our data strongly suggest that the SSB protein, together with RecO/Rad52, can be an active player in the reversal of a stalled replication fork. As fork reversal represents a potential damage avoidance pathway that allows the cells to cope with DNA blocking structures in an error-free manner (*51*), the SSB protein may contribute to genome stability.

Like the bacterial *Deinococcus radiodurans* SSB protein (*15*), T4 SSB protein more efficiently destabilizes duplexes from a structure that carries a 3′ ss tail (Figure 3A and Table 3). hRPA displays an opposite ss tail polarity preference for duplex destabilization (Table 3). In agreement with the findings of Mikhailov (*14*) but in contrast to those of Eggington et al. (*15*), our experiments show that *E. coli* SSB protein destabilizes with comparable efficiency duplexes from ds−ss junctions that carry a 5′ or 3′ ss tail. This discrepancy may stem from the length of the ss tail that is used in each study. It has been proposed that triplet repeat expansion in germ cells arises by gap repair, and more specifically after gap-filling DNA synthesis when the DNA loops comprising the trinucleotide repeats are sealed into the DNA strand by the DNA ligase (*52*). If gap repair takes place in a repetitive sequence context, duplex unwinding mediated by SSB protein can stimulate hairpin formation at the 3′ and/or 5′ side of a ss gap. SSB protein may therefore favor repetitive sequence expansions during a gap repair event and contribute to triplet repeat diseases (Figure 6B).

In agreement with the work of Jones et al. (*41*), our data show that T4 SSB protein preferentially binds model miniforks with a 5′ ss tail (Figure 1A). The same polarity tail preference is observed

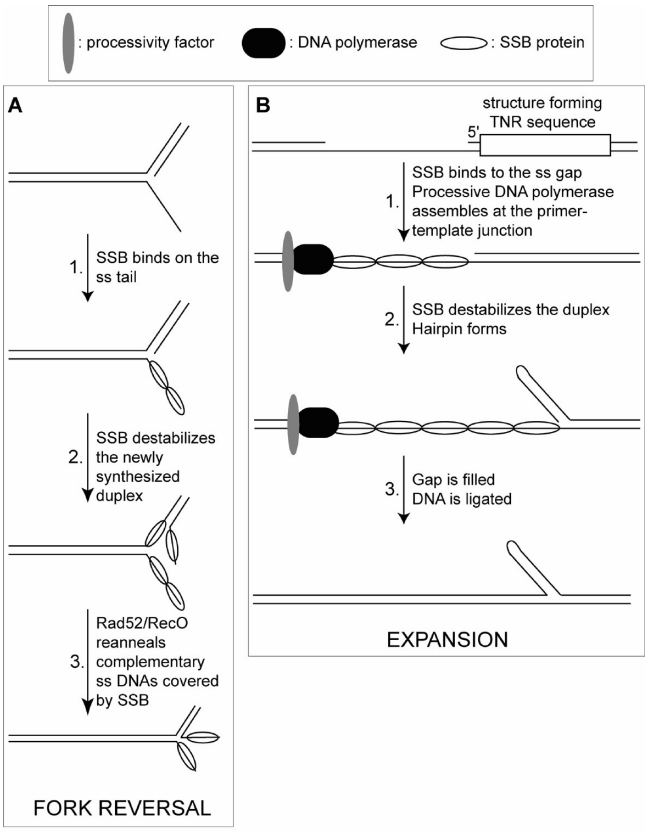

FIGURE 6: Implications of the unwinding properties of the SSB proteins in fork reversal and gap repair. Processivity factor, DNA polymerase, and SSB protein are represented as gray, black, and white ovals, respectively. (A) SSB protein promotes fork reversion with Rad52/RecO. (1) The SSB protein binds the newly exposed ss arm of the minifork. (2) The protein destabilizes the newly synthesized duplex. (3) The Rad52/RecO protein (not represented) reanneals complementary ss DNAs promoting fork reversal. (B) The SSB protein promotes TNR expansion. The ss DNA gap is located at the junction with a structure forming the TNR sequence. (1) The SSB protein binds to the ss DNA gap, and a processive DNA polymerase assembles at the primer−template junction. (2) The SSB protein destabilizes the duplex, leading to the formation of a hairpin on the 5′ side of the gap. The sequence context allows the hairpin to form. (3) DNA polymerase fills the gap, and DNA ligase joins the two DNA ends.

with ds−ss junctions, and experiments performed with short ss tails indicate that cooperativity is not required for preferential binding (Figure 4). The crystal structure of the DNA binding domain of T4 SSB protein bound to a short oligonucleotide indicates that the bases are in an unstacked and extended conformation (*24*). Recent low-energy circular dichroism and fluorescence experiments showed that the ss bases directly adjacent to a ds−ss junction with a 5′ ss tail are significantly more unstacked than those in more distant ss DNA positions (*37*). The same structural characteristic applies to the 5′ ss tail of a model minifork with two ss tails (*37*). This local structural feature might be at the origin of the preference of ss tail polarity exhibited by T4 SSB protein. *E. coli* SSB protein and hRPA exhibit binding preference for the 3′ ss tail of ds−ss junctions or miniforks (Figures 1C,D and 4B−D). Performed with a ss tail length allowing the binding of a single *E. coli* SSB protein or hRPA molecule per minifork or ds−ss junction, our experiments confirm that preference for binding a ss tail of defined polarity does not rely on cooperativity. The ss DNA in the crystal structure of the ss DNA binding domain of the p70 subunit bound to ss DNA is not reported to be unstacked or in a specific conformation (*53*). The ss bases directly adjacent to a ds−ss junction with a 3′ ss tail might be in a regular conformation that is preferentially recognized by these two proteins. Taken together, our data suggest that the 5′ ss tail of miniforks and ds−ss junctions carries a specific binding site (e.g., the few unstacked bases directly adjacent to the ds−ss junction), which is in competition with the nonspecific overlapping binding sites carried by the ss tail. Experiments performed with 30−70 junctions and T4 SSB protein (Figure 4D,E) suggest a significant difference in affinity between the specific and nonspecific binding sites, because on such substrates the nonspecific binding sites are in an ~60-fold excess relative to the specific site created by the unstacked ss bases at ds−ss junctions or miniforks.

Our data indicate that the orientation of the ss tail of a fork or a ds−ss junction that is preferentially recognized by the SSB protein is not conserved among species. ds−ss junctions with 5′ or 3′ ss overhangs can be created by ionizing radiation or by resection of blunt-ended ds breaks by 3′ → 5′ or 5′ → 3′ ds exonucleases. Rejoining of such DNA ends involves enzymes of the nonhomologous end joining pathway or of the homologous recombination pathway (for reviews, see refs (*54*−*56*)). SSB proteins are essential for the production of the recombinogenic 3′ or 5′ ss tails, and both tails can be engaged in repair after D-loop formation (*57*−*59*). Additionally, Daley and Wilson reported that ds−ss junctions with 5′ ss overhangs could be rejoined directly in a Rad52-dependent manner without conversion of the 5′ ss overhang into a 3′ ss overhang (*60*). In this repair pathway, SSB protein may assist the Rad52/RecO protein in reannealing complementary 5′ ss overhangs. In the context of a replication fork, the binding preference of T4 SSB protein for 5′ ss tails suggests preferential binding on the lagging ss template. *E. coli* SSB protein and hRPA exhibit an opposite tail polarity preference, suggesting a binding preference for a leading strand template. During unperturbed DNA replication, a role for the SSB protein on the leading ss template has still not been assigned, though in vivo data suggest that both leading and lagging strand DNA syntheses are discontinuous (*61*−*63*). The function of preferentially binding a ss tail of defined polarity is therefore not clear.

In conclusion, our data support the active participation of the SSB protein in the reversal of a stalled replication fork and in repetitive sequence instability. Whereas the potential contribution of SSB protein in fork reversal may promote genome stability, its implication during gap repair may generate genome instability. The in vivo characterization of the SSB proteins affected in their unwinding ability will certainly help confirm or refute these suggested functions.

ACKNOWLEDGMENT

We thank Ulrich Hübscher (University of Zurich) and Marc Wold (University of Iowa) for providing us with hRPA. We thank Peter H. von Hippel, Davis Jose, Steve Weitzel, and Anne-Lise Haenni for critical reading of the manuscript. We thank Claudia Göehner for subcloning the *hSSB1* gene into the pSKB3 vector and for initiating purification of hSSB1.

REFERENCES

1. Lohman, T. M., and Ferrari, M. E. (1994) *Escherichia coli* single-stranded DNA-binding protein: Multiple DNA-binding modes and cooperativities. *Annu. Rev. Biochem. 63*, 527–570.
2. Wold, M. S. (1997) Replication protein A: A heterotrimeric, single-stranded DNA-binding protein required for eukaryotic DNA metabolism. *Annu. Rev. Biochem. 66*, 61–92.

3. Binz, S. K., Sheehan, A. M., and Wold, M. S. (2004) Replication protein A phosphorylation and the cellular response to DNA damage. *DNA Repair 3*, 1015–1024.
4. Shereda, R. D., Kozlov, A. G., Lohman, T. M., Cox, M. M., and Keck, J. L. (2008) SSB as an organizer/mobilizer of genome maintenance complexes. *Crit. Rev. Biochem. Mol. Biol. 43*, 289–318.
5. Sakaguchi, K., Ishibashi, T., Uchiyama, Y., and Iwabata, K. (2009) The multi-replication protein A (RPA) system: A new perspective. *FEBS J. 276*, 943–963.
6. Broderick, S., Rehmet, K., Concannon, C., and Nasheuer, H. P. (2010) Eukaryotic single-stranded DNA binding proteins: Central factors in genome stability. *Subcell. Biochem. 50*, 143–163.
7. Richard, D. J., Bolderson, E., Cubeddu, L., Wadsworth, R. I., Savage, K., Sharma, G. G., Nicolette, M. L., Tsvetanov, S., McIlwraith, M. J., Pandita, R. K., Takeda, S., Hay, R. T., Gautier, J., West, S. C., Paull, T. T., Pandita, T. K., White, M. F., and Khanna, K. K. (2008) Single-stranded DNA-binding protein hSSB1 is critical for genomic stability. *Nature 453*, 677–681.
8. Li, Y., Bolderson, E., Kumar, R., Muniandy, P. A., Xue, Y., Richard, D. J., Seidman, M., Pandita, T. K., Khanna, K. K., and Wang, W. (2009) hSSB1 and hSSB2 form similar multiprotein complexes that participate in DNA damage response. *J. Biol. Chem. 284*, 23525–23531.
9. Jensen, D. E., Kelly, R. C., and von Hippel, P. H. (1976) DNA "melting" proteins. II. Effects of bacteriophage T4 gene 32-protein binding on the conformation and stability of nucleic acid structures. *J. Biol. Chem. 251*, 7215–7228.
10. Boehmer, P. E., and Lehman, I. R. (1993) Herpes simplex virus type 1 ICP8: Helix-destabilizing properties. *J. Virol. 67*, 711–715.
11. Georgaki, A., and Hubscher, U. (1993) DNA unwinding by replication protein A is a property of the 70 kDa subunit and is facilitated by phosphorylation of the 32 kDa subunit. *Nucleic Acids Res. 21*, 3659–3665.
12. Monaghan, A., Webster, A., and Hay, R. T. (1994) Adenovirus DNA binding protein: Helix destabilizing properties. *Nucleic Acids Res. 22*, 742–748.
13. Zijderveld, D. C., and van der Vliet, P. C. (1994) Helix-destabilizing properties of the adenovirus DNA-binding protein. *J. Virol. 68*, 1158–1164.
14. Mikhailov, V. S. (2000) Helix-destabilizing properties of the baculovirus single-stranded DNA-binding protein (LEF-3). *Virology 270*, 180–189.
15. Eggington, J. M., Kozlov, A. G., Cox, M. M., and Lohman, T. M. (2006) Polar destabilization of DNA duplexes with single-stranded overhangs by the *Deinococcus radiodurans* SSB protein. *Biochemistry 45*, 14490–14502.
16. De Vlaminck, I., Vidic, I., van Loenhout, M. T., Kanaar, R., Lebbink, J. H., and Dekker, C. (2010) Torsional regulation of hRPA-induced unwinding of double-stranded DNA. *Nucleic Acids Res. 38*, 4133–4142.
17. Treuner, K., Ramsperger, U., and Knippers, R. (1996) Replication protein A induces the unwinding of long double-stranded DNA regions. *J. Mol. Biol. 259*, 104–112.
18. Chase, J. W., and Williams, K. R. (1986) Single-stranded DNA binding proteins required for DNA replication. *Annu. Rev. Biochem. 55*, 103–136.
19. Kim, Y. T., Tabor, S., Bortner, C., Griffith, J. D., and Richardson, C. C. (1992) Purification and characterization of the bacteriophage T7 gene 2.5 protein. A single-stranded DNA-binding protein. *J. Biol. Chem. 267*, 15022–15031.
20. Shokri, L., Marintcheva, B., Richardson, C. C., Rouzina, I., and Williams, M. C. (2006) Single molecule force spectroscopy of salt-dependent bacteriophage T7 gene 2.5 protein binding to single-stranded DNA. *J. Biol. Chem. 281*, 38689–38696.
21. Shokri, L., Marintcheva, B., Eldib, M., Hanke, A., Rouzina, I., and Williams, M. C. (2008) Kinetics and thermodynamics of salt-dependent T7 gene 2.5 protein binding to single- and double-stranded DNA. *Nucleic Acids Res. 36*, 5668–5677.
22. Rouzina, I., Pant, K., Karpel, R. L., and Williams, M. C. (2005) Theory of electrostatically regulated binding of T4 gene 32 protein to single- and double-stranded DNA. *Biophys. J. 89*, 1941–1956.
23. Prigodich, R. V., Casas-Finet, J., Williams, K. R., Konigsberg, W., and Coleman, J. E. (1984) ^{1}H NMR (500 MHz) of gene 32 protein−oligonucleotide complexes. *Biochemistry 23*, 522–529.
24. Shamoo, Y., Friedman, A. M., Parsons, M. R., Konigsberg, W. H., and Steitz, T. A. (1995) Crystal structure of a replication fork single-stranded DNA binding protein (T4 gp32) complexed to DNA. *Nature 376*, 362–366, 616 (Erratum).
25. Chrysogelos, S., and Griffith, J. (1982) *Escherichia coli* single-strand binding protein organizes single-stranded DNA in nucleosome-like units. *Proc. Natl. Acad. Sci. U.S.A. 79*, 5803–5807.
26. Keshav, K. F., Chen, C., and Dutta, A. (1995) Rpa4, a homolog of the 34-kilodalton subunit of the replication protein A complex. *Mol. Cell. Biol. 15*, 3119–3128.
27. Haring, S. J., Humphreys, T. D., and Wold, M. S. (2010) A naturally occurring human RPA subunit homolog does not support DNA replication or cell-cycle progression. *Nucleic Acids Res. 38*, 846–858.
28. Kemp, M. G., Mason, A. C., Carreira, A., Reardon, J. T., Haring, S. J., Borgstahl, G. E., Kowalczykowski, S. C., Sancar, A., and Wold, M. S. (2009) An alternative form of RPA (aRPA) expressed in normal human tissues supports DNA repair. *J. Biol. Chem. 285*, 4788–4797.
29. Mason, A. C., Haring, S. J., Pryor, J. M., Staloch, C. A., Gan, T. F., and Wold, M. S. (2009) An alternative form of replication protein a prevents viral replication in vitro. *J. Biol. Chem. 284*, 5324–5331.
30. Mason, A. C., Roy, R., Simmons, D. T., and Wold, M. S. (2010) Functions of Alternative Replication Protein A in Initiation and Elongation. *Biochemistry 49*, 5919–5928.
31. Wu, M., Flynn, E. K., and Karpel, R. L. (1999) Details of the nucleic acid binding site of T4 gene 32 protein revealed by proteolysis and DNA Tm depression methods. *J. Mol. Biol. 286*, 1107–1121.
32. Bobst, E. V., Perrino, F. W., Meyer, R. R., and Bobst, A. M. (1991) An EPR study to determine the relative nucleic acid binding affinity of single-stranded DNA-binding protein from *Escherichia coli*. *Biochim. Biophys. Acta 1078*, 199–207.
33. Blackwell, L. J., and Borowiec, J. A. (1994) Human replication protein A binds single-stranded DNA in two distinct complexes. *Mol. Cell. Biol. 14*, 3993–4001.
34. de Laat, W. L., Appeldoorn, E., Sugasawa, K., Weterings, E., Jaspers, N. G., and Hoeijmakers, J. H. (1998) DNA-binding polarity of human replication protein A positions nucleases in nucleotide excision repair. *Genes Dev. 12*, 2598–2609.
35. Kolpashchikov, D. M., Khodyreva, S. N., Khlimankov, D. Y., Wold, M. S., Favre, A., and Lavrik, O. I. (2001) Polarity of human replication protein A binding to DNA. *Nucleic Acids Res. 29*, 373–379.
36. Kolpashchikov, D. M., Weisshart, K., Nasheuer, H. P., Khodyreva, S. N., Fanning, E., Favre, A., and Lavrik, O. I. (1999) Interaction of the p70 subunit of RPA with a DNA template directs p32 to the 3′-end of nascent DNA. *FEBS Lett. 450*, 131–134.
37. Jose, D., Datta, K., Johnson, N. P., and von Hippel, P. H. (2009) Spectroscopic studies of position-specific DNA "breathing" fluctuations at replication forks and primer-template junctions. *Proc. Natl. Acad. Sci. U.S.A. 106*, 4231–4236.
38. Delagoutte, E., Goellner, G. M., Guo, J., Baldacci, G., and McMurray, C. T. (2008) Single stranded DNA binding protein in vitro eliminates the orientation dependent impediment to polymerase passage on CAG/CTG repeats. *J. Biol. Chem. 283*, 13341–13356.
39. Shamoo, Y., Williams, K. R., and Konigsberg, W. H. (1988) Photochemical crosslinking of bacteriophage T4 single-stranded DNA-binding protein (gp32) to oligo-p(dT)8: Identification of phenylalanine-183 as the site of crosslinking. *Proteins 4*, 1–6.
40. van den Berg, S., Lofdahl, P. A., Hard, T., and Berglund, H. (2006) Improved solubility of TEV protease by directed evolution. *J. Biotechnol. 121*, 291–298.
41. Jones, C. E., Mueser, T. C., and Nossal, N. G. (2004) Bacteriophage T4 32 protein is required for helicase-dependent leading strand synthesis when the helicase is loaded by the T4 59 helicase-loading protein. *J. Biol. Chem. 279*, 12067–12075.
42. Iftode, C., and Borowiec, J. A. (2000) 5′ → 3′ molecular polarity of human replication protein A (hRPA) binding to pseudo-origin DNA substrates. *Biochemistry 39*, 11970–11981.
43. Shamoo, Y., Ghosaini, L. R., Keating, K. M., Williams, K. R., Sturtevant, J. M., and Konigsberg, W. H. (1989) Site-specific mutagenesis of T4 gene 32: The role of tyrosine residues in protein-nucleic acid interactions. *Biochemistry 28*, 7409–7417.
44. Chen, Y. Z., Zhuang, W., and Prohofsky, E. W. (1992) Energy flow considerations and thermal fluctuational opening of DNA base pairs at a replicating fork: Unwinding consistent with observed replication rates. *J. Biomol. Struct. Dyn. 10*, 415–427.
45. Gueron, M., and Leroy, J. L. (1995) Studies of base pair kinetics by NMR measurement of proton exchange. *Methods Enzymol. 261*, 383–413.
46. Nimonkar, A. V., Sica, R. A., and Kowalczykowski, S. C. (2009) Rad52 promotes second-end DNA capture in double-stranded break repair to form complement-stabilized joint molecules. *Proc. Natl. Acad. Sci. U.S.A. 106*, 3077–3082.
47. Shinohara, A., Shinohara, M., Ohta, T., Matsuda, S., and Ogawa, T. (1998) Rad52 forms ring structures and co-operates with RPA in single-strand DNA annealing. *Genes Cells 3*, 145–156.
48. Sugiyama, T., New, J. H., and Kowalczykowski, S. C. (1998) DNA annealing by RAD52 protein is stimulated by specific interaction with

the complex of replication protein A and single-stranded DNA. *Proc. Natl. Acad. Sci. U.S.A. 95*, 6049–6054.
49. McIlwraith, M. J., and West, S. C. (2008) DNA repair synthesis facilitates RAD52-mediated second-end capture during DSB repair. *Mol. Cell 29*, 510–516.
50. Kantake, N., Madiraju, M. V., Sugiyama, T., and Kowalczykowski, S. C. (2002) *Escherichia coli* RecO protein anneals ssDNA complexed with its cognate ssDNA-binding protein: A common step in genetic recombination. *Proc. Natl. Acad. Sci. U.S.A. 99*, 15327–15332.
51. Chang, D. J., and Cimprich, K. A. (2009) DNA damage tolerance: When it's OK to make mistakes. *Nat. Chem. Biol. 5*, 82–90.
52. Kovtun, I. V., and McMurray, C. T. (2001) Trinucleotide expansion in haploid germ cells by gap repair. *Nat. Genet. 27*, 407–411.
53. Bochkarev, A., Pfuetzner, R. A., Edwards, A. M., and Frappier, L. (1997) Structure of the single-stranded-DNA-binding domain of replication protein A bound to DNA. *Nature 385*, 176–181.
54. Hartlerode, A. J., and Scully, R. (2009) Mechanisms of double-strand break repair in somatic mammalian cells. *Biochem. J. 423*, 157–168.
55. Mahaney, B. L., Meek, K., and Lees-Miller, S. P. (2009) Repair of ionizing radiation-induced DNA double-strand breaks by non-homogous end joining. *Biochem. J. 417*, 639–650.
56. Huertas, P. (2010) DNA resection in eukaryotes: Deciding how to fix the break. *Nat. Struct. Mol. Biol. 17*, 11–16.
57. Llorente, B., and Modesti, M. (2009) Fungal BRCA2 ortholog Brh2 brings 5′ end strand invasion back on stage. *Mol. Cell 36*, 539–540.
58. Mazloum, N., and Holloman, W. K. (2009) Brh2 promotes a template-switching reaction enabling recombinational bypass of lesions during DNA synthesis. *Mol. Cell 36*, 620–630.
59. Murayama, Y., Kurokawa, Y., Mayanagi, K., and Iwasaki, H. (2008) Formation and branch migration of Holliday junctions mediated by eukaryotic recombinases. *Nature 451*, 1018–1021.
60. Daley, J. M., and Wilson, T. E. (2005) Rejoining of DNA double-strand breaks as a function of overhang length. *Mol. Cell. Biol. 25*, 896–906.
61. Amado, L., and Kuzminov, A. (2006) The replication intermediates in *Escherichia coli* are not the product of DNA processing or uracil excision. *J. Biol. Chem. 281*, 22635–22646.
62. Langston, L. D., Indiani, C., and O'Donnell, M. (2009) Whither the replisome: Emerging perspectives on the dynamic nature of the DNA replication machinery. *Cell Cycle 8*, 2686–2691.
63. Wang, T. C. (2005) Discontinuous or semi-discontinuous DNA replication in *Escherichia coli*? *BioEssays 27*, 633–636.
64. Salas, T. R., Petruseva, I., Lavrik, O., Bourdoncle, A., Mergny, J. L., Favre, A., and Saintome, C. (2006) Human replication protein A unfolds telomeric G-quadruplexes. *Nucleic Acids Res. 34*, 4857–4865.